Cancer Chemother Pharmacol
DOI 10.1007/s00280-011-1747-0

ORIGINAL ARTICLE

# Targeting autophagy enhances BO-1051-induced apoptosis in human malignant glioma cells

**Pei-Ming Chu · Li-Hsin Chen · Ming-Teh Chen · Hsin-I Ma · Tsann-Long Su · Pei-Chen Hsieh · Chian-Shiu Chien · Bo-Hua Jiang · Yu-Chih Chen · Yi-Hui Lin · Yang-Hsin Shih · Pang-Hsien Tu · Shih-Hwa Chiou**

Received: 14 July 2011 / Accepted: 13 September 2011


**Abstract**
*Purpose* BO-1051 is an N-mustard derivative that is conjugated with DNA-affinic 9-anilinoacridine. Since BO-1051 was reported to have strong anticancer activity, we investigated the effect and underlying mechanism of BO-1051 in human glioma cell lines.
*Methods* Human glioma cell lines U251MG and U87MG were studied with BO-1051 or the combination of BO-1051 and autophagic inhibitors. Growth inhibition was assessed by MTT assay. Apoptosis was measured by annexin V staining followed by flow cytometry and immunoblotting for apoptosis-related molecules. Induction of autophagy was detected by acridine orange labeling, electron microscopy, LC3 localization and its conversion. Transfection of shRNA was used to determine the involvement of Beclin1 in apoptotic cell death.
*Results* MTT assay showed that BO-1051 suppressed the viability of four glioma cell lines (U251MG, U87MG, GBM-3 and DBTRG-05MG) in a dose-dependent manner. The $IC_{50}$ values of BO-1051 for the glioma cells were significantly lower than the values for primary neurons cultures and normal fibroblast cells. Moreover, BO-1051 not only induced apoptotic cell death, but also enhanced autophagic flux via inhibition of Akt/mTOR and activation of Erk1/2. Importantly, suppression of autophagy by 3-methyladenine or bafilomycin A1 significantly increased BO-1051-induced apoptotic cell death in U251MG and U87MG cells. In addition, the proportion of apoptotic cells after BO-1051 treatment was enhanced by co-treatment with shRNA against Beclin1.
*Conclusions* BO-1051 induced both apoptosis and autophagy, and inhibition of autophagy significantly augmented the cytotoxic effect of BO-1051. Thus, a combination of BO-1051 and autophagic inhibitors offers a potentially new therapeutic modality for the treatment of malignant glioma.

**Electronic supplementary material** The online version of this article (doi:10.1007/s00280-011-1747-0) contains supplementary material, which is available to authorized users.

P.-M. Chu · H.-I. Ma (✉)
Graduate Institutes of Life Sciences, National Defense Medical Center, Taipei, Taiwan, ROC
e-mail: uf004693@mail2000.com.tw

P.-M. Chu · H.-I. Ma
Department of Neurological Surgery, Tri-Service General Hospital, No. 325, Sec. 2, Cheng-Kung Road, Taipei 114, Taiwan, ROC

L.-H. Chen · S.-H. Chiou
Institute of Pharmacology, National Yang-Ming University, Taipei, Taiwan

M.-T. Chen · Y.-H. Shih
Department of Neurosurgery, Neurological Institute, Taipei Veterans General Hospital, Taipei, Taiwan

T.-L. Su · P.-H. Tu
Institute of Biomedical Sciences, Academia Sinica, Taipei, Taiwan

P.-C. Hsieh · Y.-C. Chen · S.-H. Chiou (✉)
Department of Medical Research and Education, Taipei Veterans General Hospital, No. 201, Sec. 2, Shih-Pai Road, Taipei 112, Taiwan, ROC
e-mail: shchiou@vghtpe.gov.tw

C.-S. Chien · B.-H. Jiang
Institute of Oral Biology, National Yang-Ming University, Taipei, Taiwan

Y.-H. Lin
School of Pharmacy, China Medical University, Taichung, Taiwan

Published online: 27 September 2011

**Keywords** N-mustard · Alkylating agent · Autophagy · Apoptosis · Malignant glioma

## Introduction

Malignant glioma is the most common primary brain tumor and is associated with a high degree of morbidity and mortality. Among gliomas, glioblastoma multiforme (GBM) is the most malignant subtype. Regardless of advances in diagnosis and glioma treatment, the median life for patients with GBM is slightly greater than 1 year [1]. Removal of malignant glioma by surgical resection is usually not feasible due to highly diffuse infiltrative growth. Most patients relapse within months after complete chemo-radiotherapy. Therefore, it is urgent that effective chemotherapeutic agents for the treatment of malignant gliomas be developed.

DNA alkylating agents are commonly used to treat a variety of cancers due to the direct cytotoxic effects of these agents to produce DNA lesions [2]. Despite their clinical importance, the progress and utility of DNA-modifying drugs are often limited due to their low tumor specificity, high chemical reactivity, and the induction of bone marrow toxicity [2, 3]. To overcome these limitations, we synthesized DNA-directed alkylating agents by linking the alkylating pharmacophore to the DNA-affinity molecules [4–6]. BO-1051 is a DNA-directed alkylating compound, in which the phenyl N-mustard residue is linked to DNA-intercalating 9-anilinoacridine via a urea spacer (Fig. 1a). A previous study revealed that BO-1051 possesses broad-spectrum anti-tumor effects in vitro without cross-resistance to taxol or vinblastine [4]. Furthermore, we recently found that BO-1051 can effectively enhance the radiosensitivity of glioma cells in vitro and in vivo [7]. Besides, it has the capacity of penetrating the blood–brain barrier (unpublished data) and a long half-life in rat plasma [4]. However, the underlying mechanisms of BO-1051 activity and toxicity in the treatment of malignant glioma are still unclear.

Macroautophagy, hereafter referred to as autophagy, is a dynamic process with an important role not only in the recycling of cytoplasmic constituents to support metabolism but also in overcoming adverse conditions to prevent the accumulation of damaged, toxic proteins and organelles. A growing amount of evidence has shown that autophagy can be induced in cancer cells that are resistant radiotherapy and chemotherapy [8]. In glioma cells, autophagy appears to function as a protective mechanism against cellular stress [9–12]; however, the induction of autophagy still plays a pivotal role in cell death induced by some drugs [13–15]. Therefore, whether autophagy helps to kill glioma cells or to sustain their survival under stressful conditions remains controversial [8, 16]. To enhance the efficacy of anticancer therapy, it is critical to clarify the role of autophagy.

Recent reports suggest that autophagy and apoptosis are often induced by the same stimuli and that they share similar effectors and regulators, suggesting complex cross-talk between these two processes [17]. Apoptosis and autophagy are known to occur as a result of chemotherapy [8]. Therefore, we investigated the ability of BO-1051 to induce cytotoxicity, apoptosis, and autophagy in glioma cells. The underlying mechanisms and the relationship between autophagy and apoptosis were also examined. Elucidating the mechanism of tumor cell death may have therapeutic implications in the treatment of malignant gliomas.

## Materials and methods

### Reagents

1-{4-[bis(2-chloroethyl)amino]phenyl}-3-[2-methyl-5-(4-methylacridin-9-ylamino)phenyl]urea (BO-1051, Fig. 1a) was kindly supplied by Dr. Su, TL [4], and dissolved in DMSO. Final DMSO concentration in medium is <0.1% volume. Acridine orange (AO), 3-methyladenine (3-MA), and bafilomycin A1 (BfA1) were purchased from the Sigma Chemical Co. (St. Louis, MO, USA), and benzyloxcarbonyl-Val-Ala-Asp-fluoromethyl ketone (z-VAD-fmk) was purchased from Promega (Madison, WI, USA).

### Cell lines and culture

Human malignant glioma cell lines (U251MG, U87MG and DBTRG-05MG), medulloblastoma cell lines (D283 Med and Daoy), human astroglia cells (SVG p12), and primary GBM-3 cell line [7] were cultured in DMEM (GIBCO, Grand Island, NY, USA) supplemented with 10% fetal bovine serum (GIBCO), 4 mM glutamine, 100 units/ml penicillin, and 100 μg/mL streptomycin (GIBCO) under standard culture conditions (37°C, 95% humidified air and 5% $CO_2$). Hippocampal neurons were isolated from primary cultures of rat brains using Fu's method [18].

### Cell viability assay

Cell viability was evaluated using a modified MTT (Sigma-Aldrich) assay. Briefly, $2 \times 10^4$ cells were plated in 24-well plate and treated with different concentrations of BO-1051 (0–10 μM) for 48 h. Culture medium was then replaced with 400 μL of fresh medium containing 100 μg/mL MTT for 2 h, and the formazan crystals of the cells were then dissolved in DMSO (Sigma-Aldrich). MTT values were measured at 570 nm using a microplate reader.

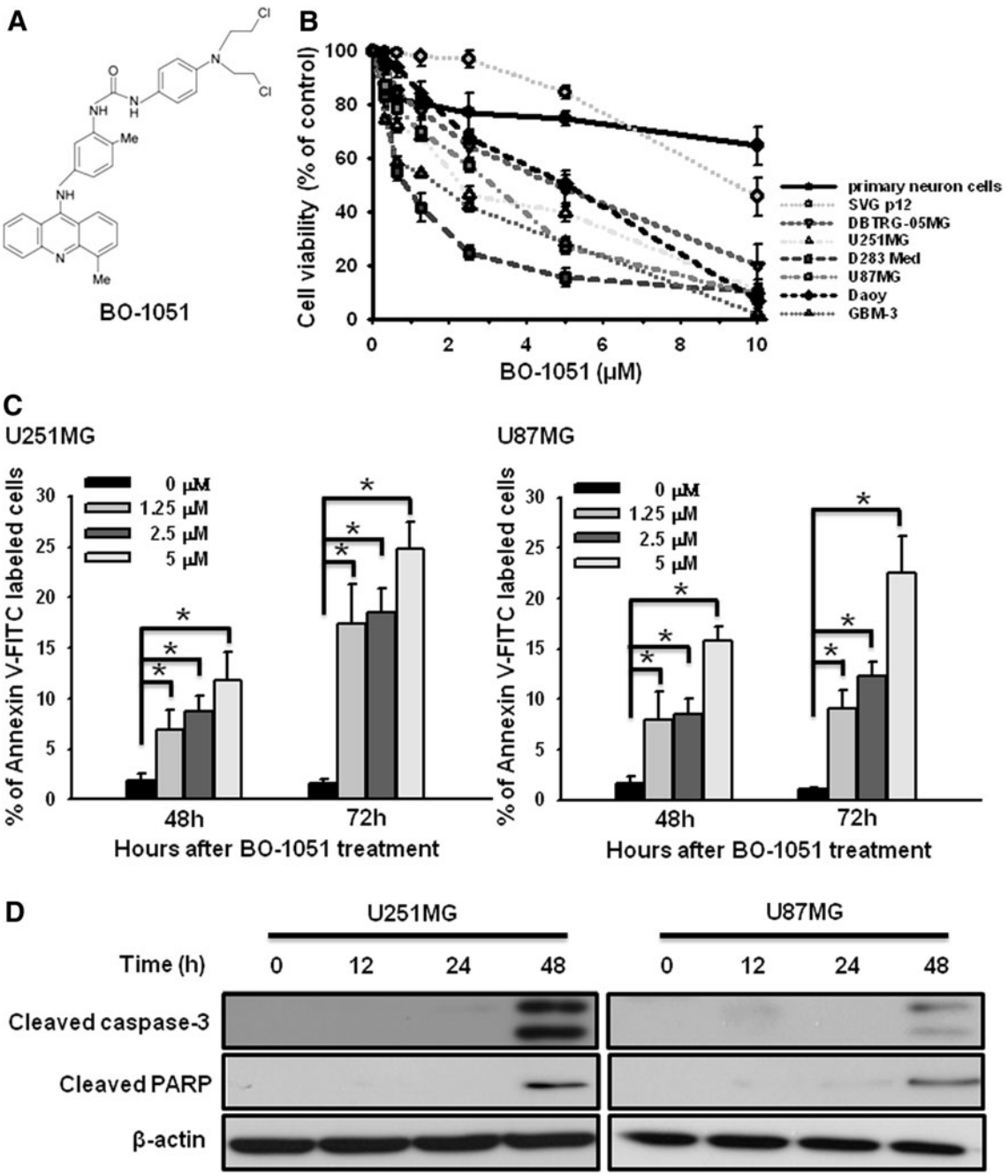


**Fig. 1** Dose-dependent effects of BO-1051 on the viability and apoptosis in U251MG and U87MG cells. **a** The chemical structure of BO-1051. **b** Malignant glioma (U87MG, U251MG, GBM-3 and DBTRG-05MG), medulloblastoma (D283 Med and Daoy), SVG p12 cells, and primary neurons were treated with BO-1051 (0–10 μM) for 48 h, and cell viability was determined by MTT assay. **c** U251MG and U87MG cells were treated with different concentrations of BO-1051 for the indicated times. Cells were harvested and stained with annexin V-FITC and PI followed by flow cytometric analysis. $^*P < 0.05$. **d** U251MG and U87MG cells were treated with DMSO or 2.5 μM BO-1051 for the indicated time, and cell lysate was subjected to Western blot analysis using antibodies against cleaved caspase-3 and cleaved PARP. *β*-actin expression was measured as a loading control

The absorbance of the untreated cells represented 100% viability. The 50% inhibitory concentration ($IC_{50}$) was the concentration that caused a 50% decrease in the optical density with respect to untreated cells.

## Apoptosis detection assay

Apoptosis in BO-1051-treated glioma cells was detected using a FITC-conjugated annexin V kit (BD Biosciences,

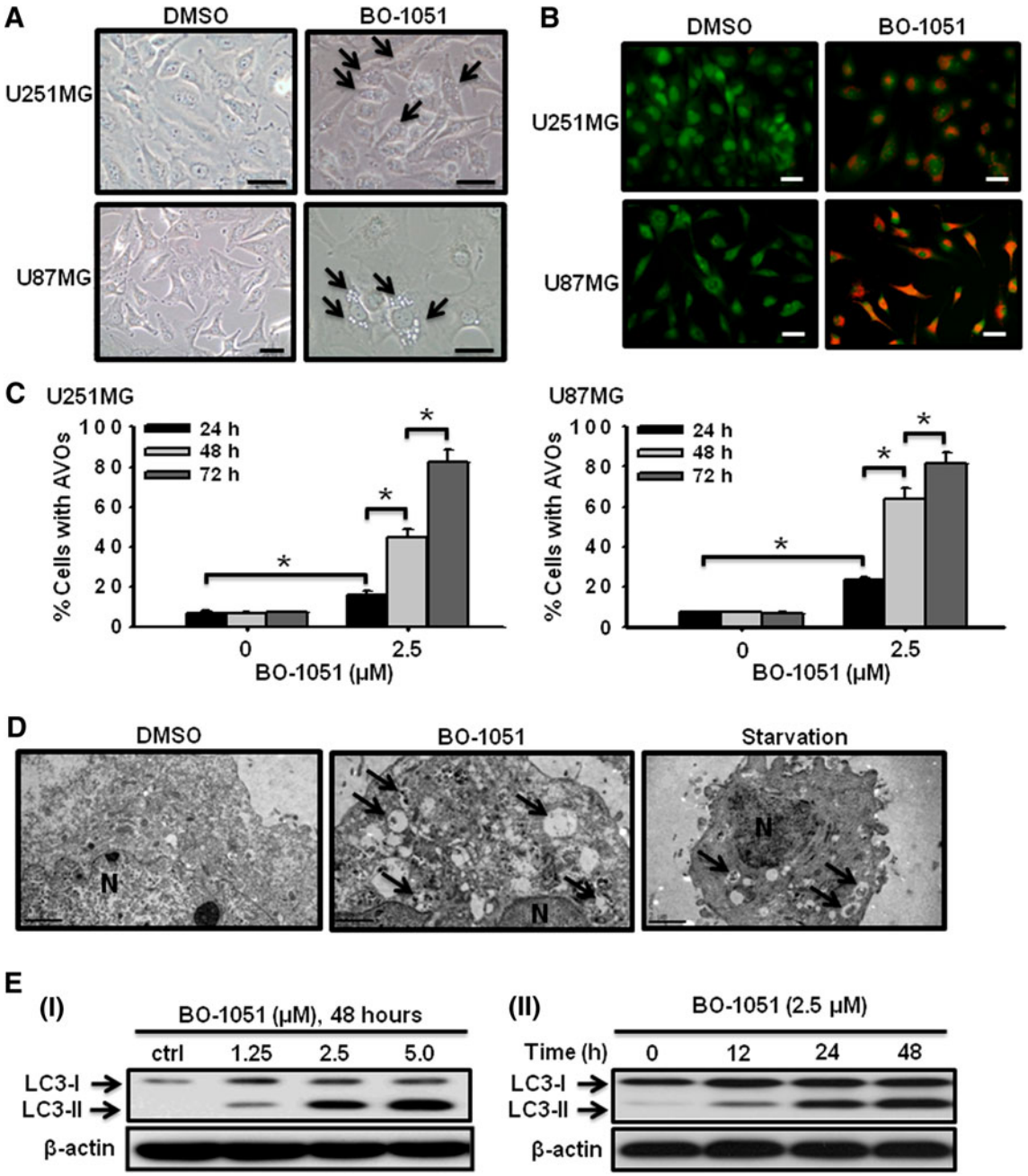


**Fig. 2** BO-1051 induced autophagy in U251MG and U87MG cells. **a**, **b** Cells were incubated with DMSO or 2.5 μM BO-1051 for 48 h. **a** Representative images were taken on a phase-contrast microscope. *Arrows* denote vacuoles within the cells. *Scale bars* 50 μm. **b**, **c** Glioma cells were treated with 2.5 μM BO-1051 for 48 h and stained with AO. Cells were then observed using a fluorescence microscope (**b**). *Scale bars* 20 μm. The percentage of cells with AVOs was quantified by flow cytometry (**c**). $*P < 0.05$. **d** Ultrastructural features of U251MG cells in nutrient-free conditions (starvation for 12 h) or treated with BO-1051 (2.5 μM) for 48 h. Cells were harvested, fixed, and observed using an electron microscope. *N* represents the nucleus, and *arrows* indicate autophagic vacuoles. *Scale bar* 2 μm. **e** U251MG cells were treated with various concentrations of BO-1051 for 48 h (I) or treated with 2.5 μM BO-1051 for indicated the time (II). Whole cell lysate was subjected to a Western blot analysis of the conversion of LC3-I to LC3-II. *β*-actin and GAPDH expression were measured as loading controls

Bedford, MA, USA). Inhibitors of autophagy, such as 3-MA (5 mM) and BfA1 (10 nM), were added to the culture medium 1 h before BO-1051 treatment. After treatment, cells were harvested and stained with annexin V-FITC and PI according to the manufacturer's instructions. Cell death was measured using a flow cytometer and analyzed using CellQuest software (Becton–Dickinson).

### Detection and quantification of acidic vesicular organelles using acridine orange staining

Autophagy is characterized by the formation of acidic vesicular organelles (AVOs) [19]. To detect and quantify AVOs, we stained them with 1.0 μg/mL acridine orange (AO) for 30 min. Images were obtained using a fluorescence microscope. In addition, green (510–530 nm) and red (>650 nm) fluorescence, which was illuminated with blue (488 nm) light excitation, was measured using FACSCalibur (Becton–Dickinson) and analyzed using CellQuest software. The fluorescence intensity is proportional to the degree of acidity and/or the volume of the cellular acidic compartment.

### Transmission electron microscopy

Cells were fixed with a solution containing ice-cold glutaraldehyde (3% in 0.1 M cacodylate buffer (pH 7.4)) for 30 min. After fixation, the samples were post-fixed in 1% OsO4 and embedded in Epon. Ultrathin sections were cut and stained with uranyl acetate and lead citrate. Representative areas were observed under a transmission electron microscope (TEM; JEOL JEM-2000EXII).

### Immunofluorescence of microtubule-associated LC3B

Cells were seeded on cover slips and treated with or without BO-1051 for the indicated time. After treatment, cells were fixed with 4% paraformaldehyde, permeabilized with 0.1% Triton X-100 (Sigma), stained with an anti-LC-3 antibody (Cell Signaling Technology, Beverly, MA, USA), and visualized with goat anti-rabbit IgG conjugated with FITC. Cover slips were then mounted with an anti-fade solution (Dako Corp.; Carpinteria, CA), and cells were examined using a confocal laser scanning microscope (CLSM, LSM 5 Pascal, Zeiss, Germany) with a 63X oil objective (NA = 1.4, Zeiss) on an inverted microscope (Axiovert 200 M, Zeiss). To excite the FITC and PI, a 488 nm and a 543 nm laser were used, respectively.

### Western blot analysis

Western blot analysis was performed as described previously [20]. The protein concentration of cell lysate was measured using a protein assay kit (Bio-Rad Laboratories, Hercules, CA, USA). Twenty micrograms of total protein was separated by SDS–PAGE and transferred to nitrocellulose membranes (Pall Corporation, MI, USA). Membranes were probed with antibodies against LC3 (Cell Signaling Technology), Beclin1 (Sigma), p62 (Progen biotechnik, Heidelberg, Germany), cleaved PARP, cleaved caspase-3, phospho-Akt, Akt, phospho-mTOR, mTOR, phospho-p70S6K, p70S6K, phospho-4EBP1, 4EBP1, phospho-ERK1/2, ERK1/2 (Cell Signaling Technology), and $\beta$-actin (Millipore Corporation, Milford, MA, USA).

### Assessment of the mitochondrial membrane potential

Changes in the mitochondrial membrane potential were measured using tetramethylrhodamine, ethyl ester per chlorate (TMRE, Molecular Probe Inc., Eugene, OR, USA) coupled with flow cytometry. Glioma cells were treated with BO-1051 at different concentrations for 48 h. After treatment, cells were stained with 200 nM TMRE for 20 min at 37°C and collected for fluorescence analysis.

### shLuc and shBeclin1 expression constructs and lentiviral transduction

Lentiviral plasmids harboring a puromycin-resistance gene and Beclin1-targeted shRNA (TRCN0000033549 (shBeclin1 A01) and TRCN0000033550 (shBeclin1 B01)) were obtained from the National RNAi Core Facility at Academia Sinica, Taiwan. The sequences of shBeclin1 A01 and shBeclin1 B01 correspond to nucleotides 889–909 and 984–1004 of the Beclin1 mRNA, respectively [20]. U251MG cells were plated and transduced with shBeclin1 A01, shBeclin1 B01, or control plasmid shLuc (pLKO.1-shLuc) for 48 h. Stable clones were established by puromycin selection (2 μg/mL) for at least 14 days, and the knockdown efficiency was evaluated by Western blot analysis.

### Statistical analysis

Values are expressed as the mean ± standard error of the mean. All experiments were repeated at least 3 times. Statistical analysis was performed using an unpaired Student's $t$ test, and a $P$ value of less than 0.05 was considered statistically significant.

## Results

### Dose-dependent effects of BO-1051 on the viability and apoptosis in glioma cells

BO-1051, a phenyl N-mustard-9-anilinoacridine conjugate, induces significant DNA inter-strand cross-linking and possesses potential anticancer activity [4, 7]. The underlying mechanism of BO-1051-induced cell death, however, has not been determined in glioma. To examine the antitumor effects of BO-1051, malignant glioma cell lines (U87MG, U251MG, GBM-3 and DBTRG-05MG), medulloblastoma cell lines (D283 Med and Daoy), human astroglia cell line (SVG p12), and primary neuron cells

were treated with BO-1051 at concentrations ranging from 0 to 10 μM for 48 h, and cell viability was determined using a MTT assay. As shown in Fig. 1b, BO-1051 significantly inhibited cell viability in every type of tumor cell in a dose-dependent manner. The $IC_{50}$ values for brain tumor cells ($IC_{50}$: 0.91–4.38 μM) were significantly lower than the values for human astroglia cells, primary neuron cells, and normal fibroblasts ($IC_{50}$: >10 μM) (Supplemental table 1).

After 48 h of treatment with BO-1051, glioma cells displayed an apoptotic morphology including plasma membrane blebbing and cell shrinkage. Early apoptosis was detected in U251MG and U87MG cells treated with BO-1051 by annexin V-FITC staining. As shown in Fig. 1c, treatment with BO-1051 induced cellular apoptosis in a dose- and time-dependent manner. A significant number of apoptotic cells were detected in U251MG and U87MG cells after 48 and 72 h of BO-1051 treatment, whereas less than 5% apoptotic cells was detected after a short-term treatment (data not shown). Consistent with this observation, the cleaved form of caspase-3 and PARP was also detected in U251MG and U87MG cells treated with BO-1051 for 48 h (Fig. 1d). These results indicated that apoptosis was induced by BO-1051 in glioma cells.

## Induction of autophagy in BO-1051-treated glioma cells

Notably, treatment of U251MG and U87MG cells for 48 h with 2.5 μM BO-1051 resulted in the vacuolization of the cytoplasm (Fig. 2a), and the number and size of vacuoles increased gradually with time. Consistent with above observations, an increased side scatter profile was observed in BO-1051-treated cells by flow cytometry, revealing dramatic changes in the cellular granularity (data not shown). Previous studies showed that malignant glioma cells undergo autophagy in response to radiation or chemotherapeutic agents, such as temozolomide and arsenic trioxide [11, 21–24]. To assess whether BO-1051-induced vacuoles were autophagic, we examined the autophagy-inducing effects of BO-1051 using the following assays. First, we determined AVO formation in BO-1051-treated cells using AO staining. As shown in Fig. 2b, vehicle-treated (DMSO) U251MG and U87MG cells displayed diffuse green fluorescence with minimal red fluorescence. In BO-1051-treated cells, numerous AVOs, characterized by red fluorescence, accumulated in acidic compartments, and formed dot-like structures, which were distributed within the cytoplasm and localized to perinuclear regions (Fig. 2b). Moreover, flow cytometry was performed to quantify AVO formation in BO-1051-treated cells. As indicated in Fig. 2c, the number of AVOs was significantly increased in U251MG and U87MG cells treated with BO-1051 in a time-dependent manner as compared to control cells. In addition, ultra-structure analysis of BO-1051-treated U251MG cells was performed using a TEM. As shown in Fig. 2d, autophagic vacuoles with residual digested materials similar to starvation-induced autophagosome were observed in BO-1051-treated U251MG cells, whereas DMSO-treated cells lacked these features. Furthermore, we performed Western blot analysis to evaluate the amount of LC3-I and LC3-II, an indicator of autophagy, because the conversion of the LC3 from the unconjugated form (LC3-I, 18 kDa) to the phosphatidylethanolamine-conjugated form (LC3-II, 16 kDa) correlates with autophagosome formation. The data indicated a dose- and time-dependent increase in autophagy-specific LC3-II in BO-1051-treated U251MG cells compared with control cells (Fig. 2e). Together, these results indicate that BO-1051 indeed induced autophagy, which was manifested in cells by vacuolization and LC3-II accumulation.

**Fig. 3** The effects of autophagic inhibitors, 3-methyladenine (3-MA), and bafilomycin A1 (BfA1), on BO-1051-induced autophagy. **a–c** Inhibitory effects of 3-MA (5 mM) or BfA1 (10 nM) on BO-1051-induced AVO formation in U251MG cells. Cells were treated with 3-MA (I) or BfA1 (II) 1 h before the addition of 2.5 μM BO-1051. After 48 h, cells were stained with AO followed by observation under a fluorescence microscope (**a**) or quantification by flow cytometry (**b**, **c**). FL1-H indicates green color intensity, whereas FL3-H shows *red* color intensity. $*P < 0.05$. *Scale bars* 20 μm. **d** 3-MA suppressed BO-1051-induced LC3 puncta formation. U251MG cells were pretreated with 3-MA (5 mM) 1 h prior to treatment with BO-1051 (2.5 μM) for 48 h followed by immunostaining of LC3 (*green fluorescence*) and PI (*red fluorescence*). *Scale bars* 20 μm. **e** 3-MA treatment reduced BO-1051-dependent conversion of LC3-I to LC3-II. U251MG cells were pretreated with 3-MA 1 h before BO-1051 treatment. After 48 h incubation, cells were lysed and Western blot analysis was performed to determine LC3 expression. **f** U251MG cells were treated with BfA1 1 h before the addition of 2.5 μM BO-1051. After 48 h or indicated time, Western blot analysis was performed to measure LC3 and p62/SQSTM1 expression

## Effects of 3-methyladenine (3-MA) or bafilomycin A1 (BfA1) on BO-1051-induced autophagy in malignant glioma cells

Next, we investigated whether BO-1051-induced autophagy could be inhibited by the autophagy inhibitors 3-MA and BfA1, which inhibit autophagic sequestration during early stage autopahgy and inhibit the fusion of the autophagosome and lysosome during late stage autophagy, respectively [8]. U251MG cells co-treated with BO-1051 and an autophagy inhibitor were stained for AO. As shown in Fig. 3a, treatment with 3-MA or BfA1 significantly attenuated BO-1051-induced AVO formation. The inhibitory effects of 3-MA (Fig. 3b) and BfA1 (data not shown) on the proportion of AO-positive cells were analyzed by flow cytometry. Nearly half of the U251MG cells treated with BO-1051for 48 h contained AVOs (44.4%), while only 7% of DMSO-treated

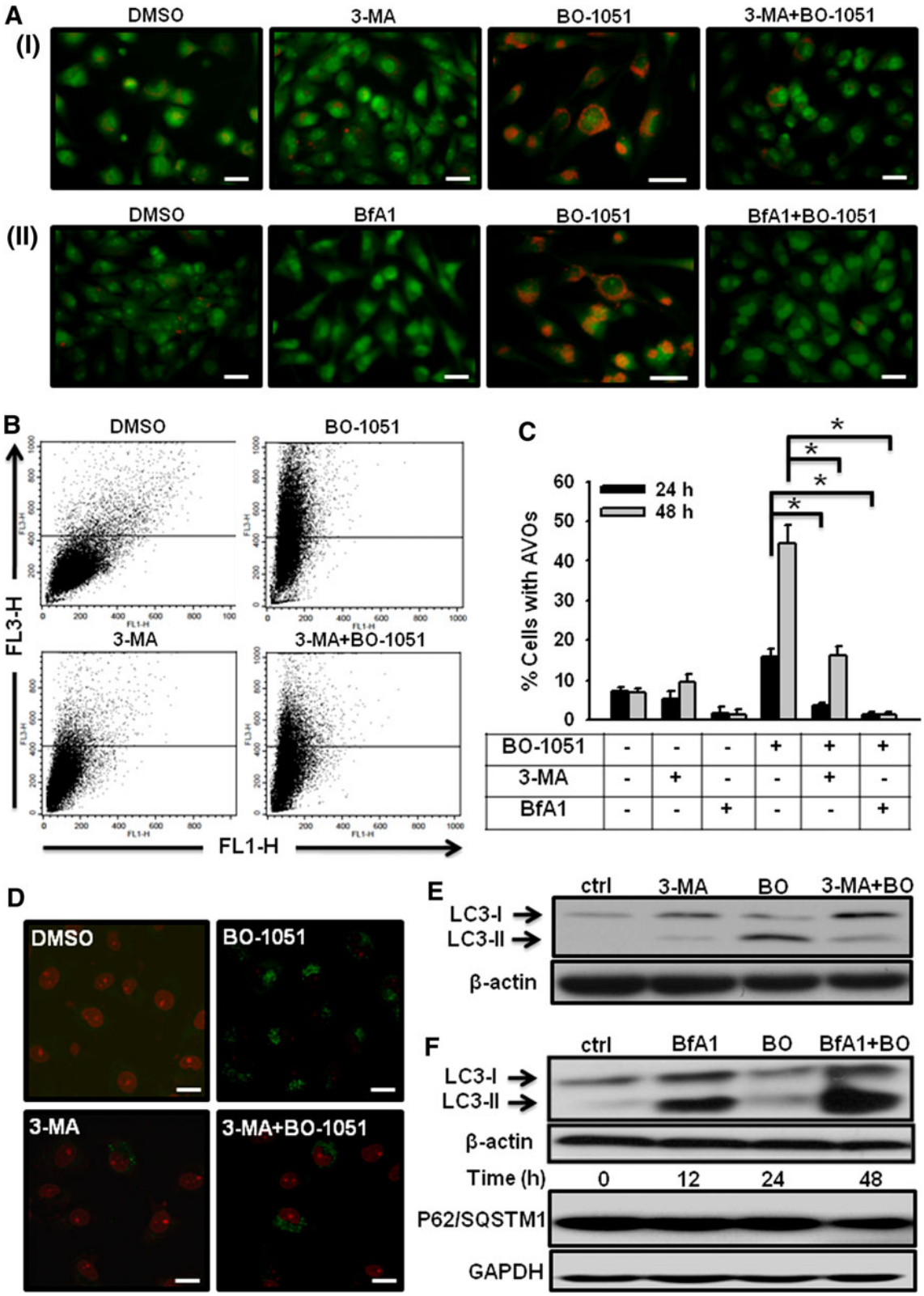


cells showed AVO formation. The percentage of AVO-harboring cells was decreased to 16.0 and 1.4% in the presence of 3-MA and BfA1 for 48 h, respectively (Fig. 3c). The inhibitory effects of 3-MA and BfA1 were also observed after 24-h incubation. To further study the effects of autophagic inhibitors on BO-1051 treatment, LC3 punctations,

which are localized to the autophagosome membrane, were detected by immunofluorescence. As demonstrated by a confocal fluorescence microscope in Fig. 3d, immunostaining showed a homogenous cytosolic distribution of LC3 in the DMSO-treated U251MG cells. However, a predominant LC3 signal was detected in the cytoplasm, where it exhibited a punctate pattern after treatment with 2.5 μM BO-1051 for 48 h. The combination of BO-1051 and 3-MA reduced LC3 puncta formation. Consistent with this data, Western blot analysis of LC3-II conversion demonstrated that the BO-1051-dependent effects were inhibited by 3-MA (Fig. 3e). To determine whether the BO-1051-dependent effects on the accumulation of LC3 puncta and LC3-II were due to increased autophagy or inhibition of autophagosome degradation [25], the lysosomal acidification blocker BfA1 was used to inhibit autophagic flux. Whereas proteolysis inhibition by BfA1 increased LC3-II levels in U251MG cells, co-treatment with BO-1051 and BfA1 enhanced the BO-1051-triggered conversion of LC3-II (Fig. 3f). In addition, treatment with BO-1051 reduced the expression of p62 (Fig. 3f), a protein selectively degraded during autophagy [26]. These observations indicate that BO-1051 increased autophagic flux as opposed to the inhibition of LC3-II degradation.

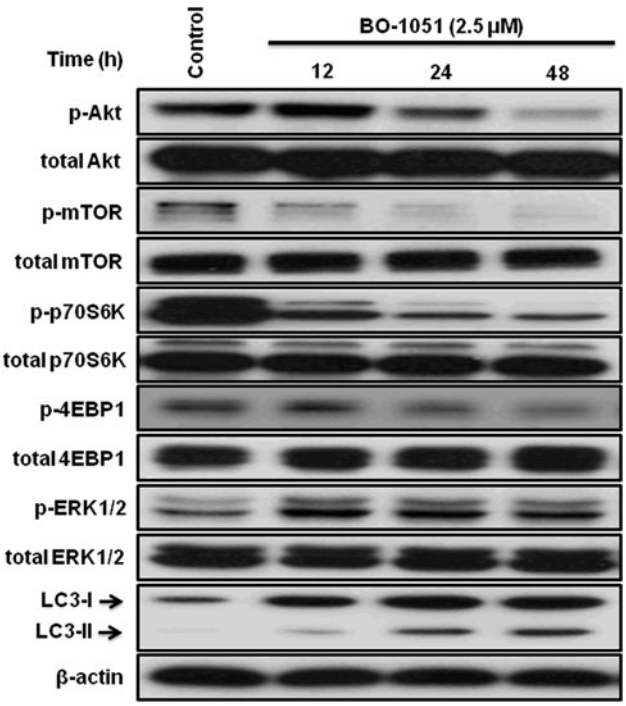


**Fig. 4** BO-1051-induced autophagy in U251MG cells, by the suppression of Akt/mTOR and activation of Erk1/2. Cells were exposed to 2.5 μM BO-1051 for 12, 24, or 48 h, and the activity of Akt/mTOR and Erk1/2 as well as LC3 conversion was analyzed by Western blot analysis

## BO-1051 inhibits Akt/mTOR signaling and activates Erk1/2 signaling

To understand how autophagy is activated during BO-1051 treatment, we examined the activity of Akt/mTOR, a negative regulator of autophagy. We assessed the phosphorylation status of Akt/mTOR as well as two well-characterized substrates of mTOR, p70S6K and 4EBP1 by Western blot analysis. As demonstrated in Fig. 4, treatment with BO-1051 for 12–48 h significantly suppressed the phosphorylation of Akt at Ser 473, phosphorylation of mTOR at Ser 2448, phosphorylation of p70S6K at Thr 389, and phosphorylation of 4EBP1 at Thr 37/46 in U251MG cells. We also analyzed the Erk1/2 signaling pathway, which is reported to positively regulate autophagy [27]. As shown in Fig. 4, increased phosphorylated Erk1/2 was detected in U251MG cells after treatment with BO-1051, suggesting increased activation of Erk1/2 signaling. Taken together, these results demonstrated that BO-1051 induced autophagy in U251MG cells by inhibiting Akt/mTOR and by activating Erk1/2.

## Pharmacologic inhibition of autophagy and knockdown of Beclin1 enhanced BO-1051-induced apoptosis

A considerable number of studies report that autophagy plays a role in cytoprotection in response to nutrient deprivation and causes cell death in response to a variety of chemotherapeutic agents [8, 28]. The exact role of autophagy and the relationship between autophagy and apoptosis remain poorly understood. To elucidate the functional role of autophagy in BO-1051-induced cell death, cells were treated with autophagy inhibitors and apoptosis was determined by annexin V-FITC and PI staining. The percentage of annexin V-positive cells induced by BO-1051 was significantly higher in the presence of 3-MA (Fig. 5a) or BfA1 (Fig. 5b); these effects were suppressed by the apoptosis inhibitor z-VAD-fmk. Moreover, BO-1051-induced cleavage of caspase-3 and PARP was further increased by treatment with 3-MA (Fig. 5c), indicating that the inhibition of autophagy enhanced BO-1051-induced apoptosis.

During apoptosis, mitochondrial dysfunction results in a reduced mitochondrial membrane potential. Because inhibition of autophagy enhanced BO-1051-induced apoptosis, the mitochondrial membrane potential was examined by TMRE staining followed by FACS analysis. Membrane potential-driven TMRE accumulation within the inner membrane of healthy mitochondria results in an increase in TMRE-associated orange fluorescence. Detection of the loss of orange-red fluorescence in TMRE stained cells is a reliable method of assessing apoptosis. As shown in Fig. 5d, e, BO-1051 treatment induced approximately 14% loss of orange-red fluorescence compared with DMSO-treated

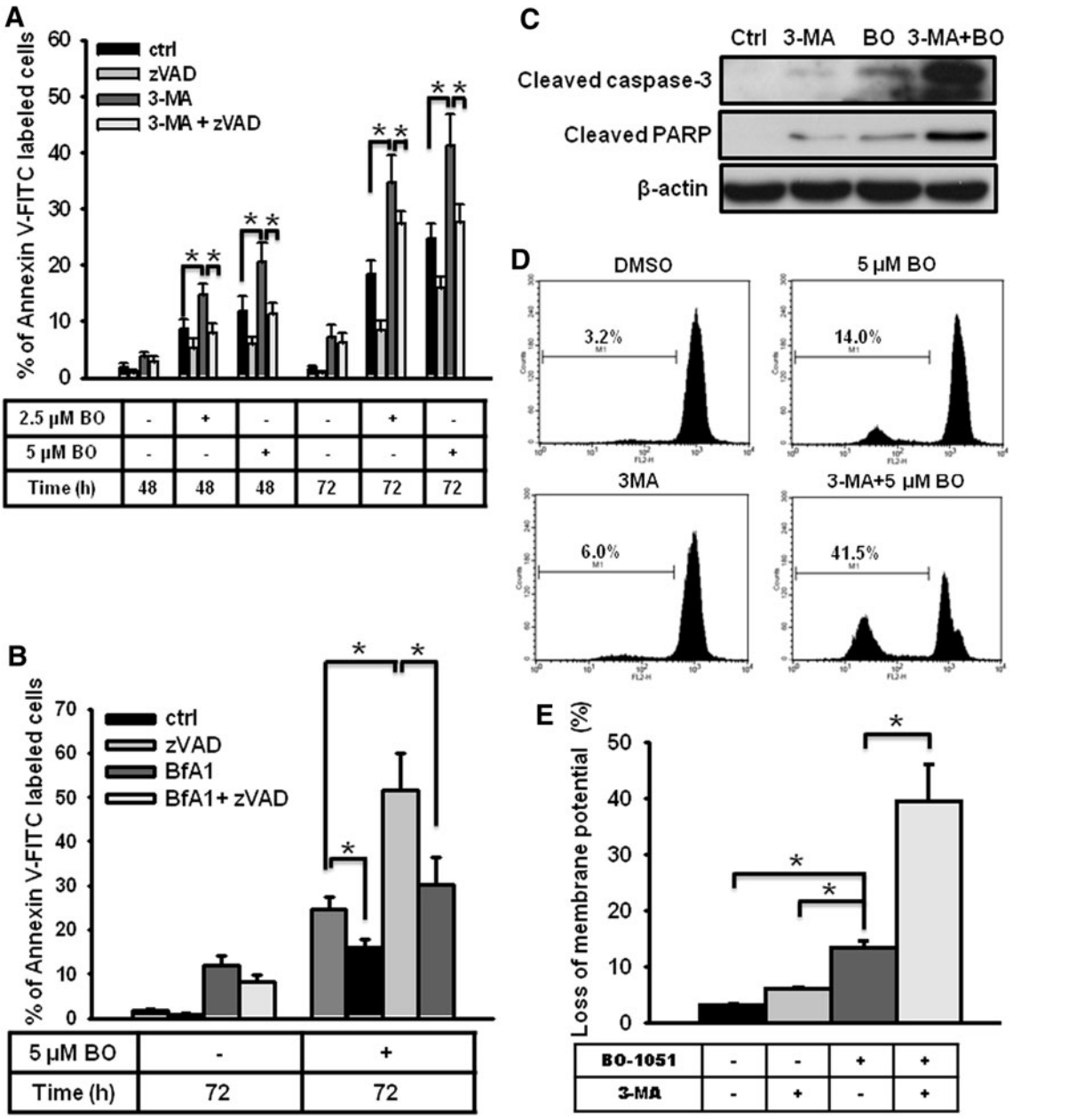


**Fig. 5** Pharmacologic inhibition of autophagy enhanced BO-1051-induced apoptosis and reduced the mitochondrial membrane potential in U251MG cells. **a**, **b** The effects of the autophagy inhibitors 3-MA and BfA1 on BO-1051-induced apoptotic cell death were determined. U251MG cells were treated with various combinations of drug for the indicated time. 3-MA (5 mM), BfA1 (10 nM), and zVAD-fmk (25 μM) were added to the culture medium 1 h before BO-1051 (2.5 or 5.0 μM) treatment. After 48 or 72 h, the cells were collected and stained with annexin V-FITC and PI followed by flow cytometric analysis. $*P < 0.05$. **c** U251MG cells were treated with 3-MA, BO-1051 (2.5 μM), or both for 48 h. Cell lysates were prepared and subjected to Western blot analysis using antibodies against cleaved caspase-3, cleaved PARP, and $\beta$-actin. **d** U251MG cells were treated with BO-1051(5 μM), 3-MA, or both for 48 h and stained with TMRE. The mitochondrial membrane potential was then analyzed by flow cytometry. **e** Quantitative data of (**d**). $*P < 0.05$

cells, whereas a significant percentage of U251MG cell population (~40%) shifted toward the lower level of fluorescence after co-treatment with BO-1051 and 3-MA (Fig. 5d) or BfA1 (data not shown). Similar results were also observed in U87MG cells (Supplemental Fig. 1).

Because chemical inhibitors of autophagy can have non-specific effects, manipulating the expression of autophagy-related genes by shRNA allows more specific characterization of the relationship between autophagy and apoptosis. We stably transduced cells with plasmids

(shBeclin1 A01 or shBeclin1 B01) encoding the antisense RNA sequence for Beclin1, an *Atg* gene essential for autophagy. Western blot analysis demonstrated that RNA interference caused a significant reduction of Beclin1 protein expression in U251MG cells. Beclin1-knockdown cells treated with BO-1051 had elevated expression of cleaved caspase-3 and PARP compared with control cells, and the appearance of these apoptosis-related proteins was further suppressed by treatment with z-VAD-fmk (Fig. 6a). Consistent with these data, annexin V-FITC staining of Beclin1 knockdown cells increased with BO-1051 treatment (Fig. 6b). Furthermore, TMRE staining was performed to determine the effect of Beclin1 knockdown on the BO-1051-induced loss of mitochondrial membrane potential. As shown in Fig. 6c, d, U251MG cells with a stable knockdown of Beclin1 had a marked response to BO-1051 and dramatic loss of mitochondrial membrane potential, suggesting that knockdown of Beclin1 enhanced the toxicity of BO-1051. Taken together, these results indicate that autophagy is cytoprotective in glioma cells in response to BO-1051 treatment.

**Fig. 6** Knockdown of Beclin1 expression enhanced BO-1051-induced apoptosis in U251MG cells. **a** Cells stably expressing shLuc or shBeclin1 B01 were generated through puromycin selection. Stable clones were treated with z-VAD-fmk (25 μM), BO-1051 (5 μM), or both for 48 h, and the expression of Beclin1, cleaved caspase-3, and cleaved PARP was examined by Western blot analysis. **b** U251MG clones stably over-expressing shLuc, shBeclin1 A01, or shBeclin1 B01 were treated with BO-1051 and z-VAD-fmk as indicated in the table. Apoptotic cells were detected using annexin V-FITC and PI staining and analyzed using flow cytometry. $*P < 0.05$. **c** The mitochondrial membrane potential of cells from **b** as assessed by TMRE staining and analyzed using flow cytometry. **d** Quantitation of (**c**). $*P < 0.05$

## Discussion

Although toxicity and resistance are major limitations associated with alkylating drug chemotherapy, these agents remain the first-line treatment for a variety of cancers. Newly designed alkylating agents should be selective for cancer cells to minimize toxicity. BO-1051, a DNA-affinic 9-anilinoacridine conjugate, was designed with increased affinity and specificity for DNA in cancer cells. This compound has a broad spectrum of anticancer activities in vitro and in vivo [4]. In this study, BO-1051 induced high tumor-specific cytotoxicity and apoptotic cell death. Furthermore, BO-1051-mediated autophagy was characterized by the formation of membranous vacuoles containing residual digested materials, the formation of AVOs, the induction of autophagosome-associated LC3-II, and the accumulation of LC3-II punctation. Importantly, BO-1051-induced autophagy protected glioma cells from apoptotic cell death.

Although autophagy may be protective against nutrient starvation by recycling macromolecules and removing damaged mitochondria and other organelles, it can also result in cell death, designated as programmed cell death type II or autophagic cell death [29]. Moreover, recent studies reported that once cancer cells are exposed to stresses such as chemotherapy and radiation therapy, a high rate of autophagy is observed as cells adapt to the adverse conditions; however, the molecular mechanisms of this process have not been fully elucidated [8, 30]. In our study, we provide evidence that the BO-1051-triggered stress simultaneously evoked two different responses in glioma cells: apoptotic cell death and autophagy. These data are consistent with previous studies showing that both autophagy and apoptotic cell death coexist after treatment with drugs such as arsenic trioxide [31–34]. However, the relationship between autophagy and apoptosis in response to anticancer agents is still debated because there is an overlap between autophagic and apoptotic pathways [17].

Our data revealed that abrogation of autophagy by inhibitors, such as 3-MA and BfA1, or by shRNA knockdown of beclin1, an autophagy-related molecule, remarkably exacerbated cleaved caspase-3 and PARP as well as apoptotic cell death. Although Kanzawa et al. reported that inhibition of autophagy at different stages has opposite effects on cell survival following temozolomide treatment [11], we found that inhibition of autophagy at either early or late stage leads to enhanced apoptosis in our research. The observed differences may result from great variety existing in the distinct cellular characteristics, as well as in the responses induced by different anticancer drugs. Besides, our results agree with previous reports that autophagy antagonizes or delays the onset of apoptosis in breast cancer cells following DNA damage [35] and that the inhibition of autophagy increases cell sensitivity to various therapies, including ionizing irradiation and treatment with cisplatin, sulforaphane, and alkylating drugs [19, 22, 35–38]. From this perspective, pharmaceutical inhibition of autophagy may represent a new anticancer treatment strategy. For example, chloroquine, an autophagy inhibitor, prolongs median survival and decreases the rate of death for patients undergoing GBM treatment [39]. Future experiments are required to extend our in vitro results and evaluate the effect of BO-1051 treatment in mouse xenograft models.

Herman-Antosiewicz et al. showed that sulforaphane-induced autophagy sequesters mitochondria in autophagosomes, resulting in delayed cytochrome c release and intrinsic caspase cascade activation [37]. In response to weak stressors, cells can prevent mitochondria depolarization effectively. However, in the presence of elevated

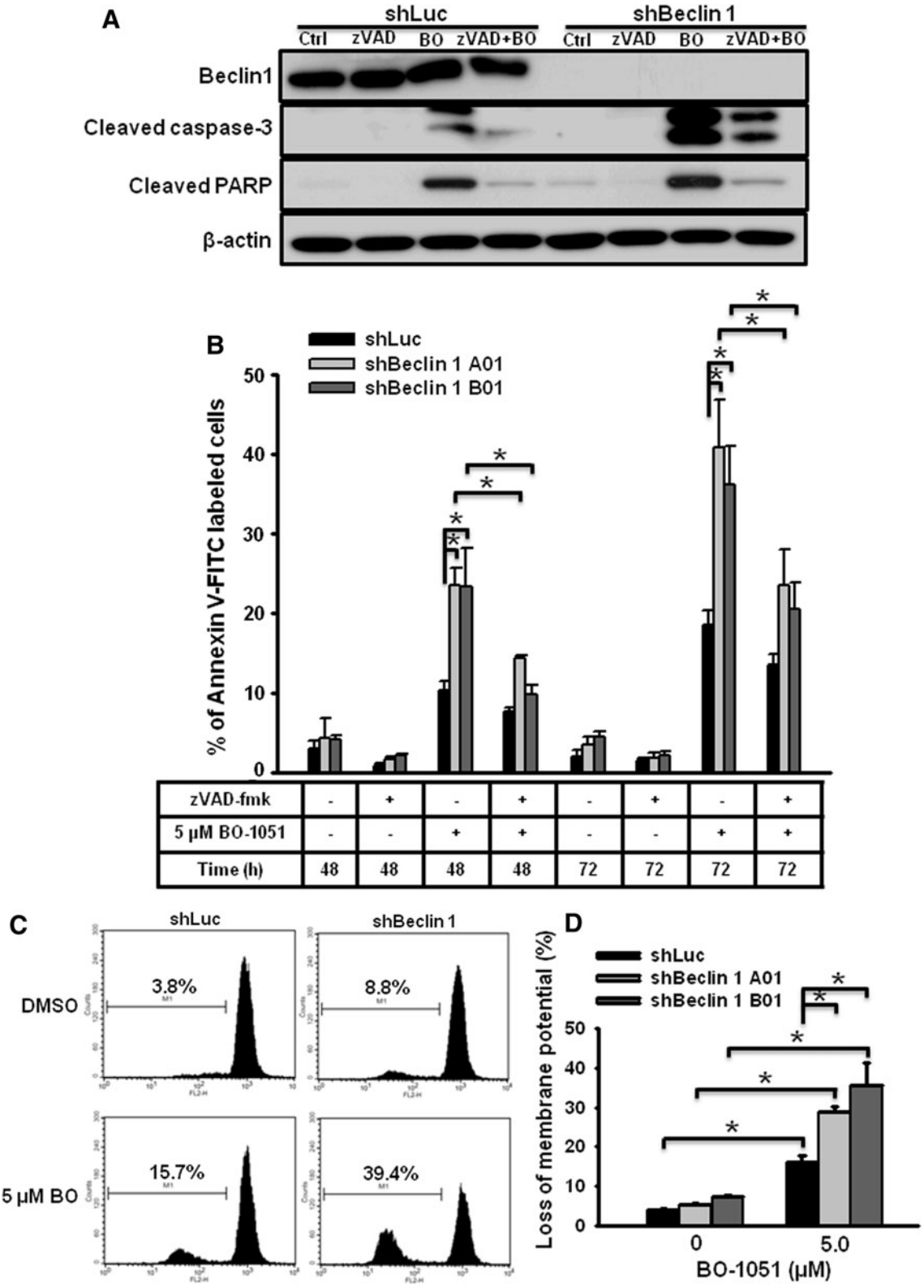


cell stress, mitochondria depolarization leads to the release of apoptotic molecules followed by programmed cell death. In addition, inhibition of temozolomide-induced autophagy by BfA1 causes mitochondrial permeabilization and the release of cathepsin D and results in apoptosis [11]. In our study, treatment with BO-1051 disrupted the mitochondrial

membrane potential in glioma cells. Moreover, when autophagy is suppressed, enhanced apoptotic cell death is coupled with an increase in the dissipation of the mitochondrial membrane potential. Therefore, it appears that inhibition of autophagy prevents the removal of damaged mitochondria, thereby accelerating apoptotic cell death.

Reactive oxygen species (ROS) are multifaceted signaling molecules implicated in a variety of cellular programs under physiological and pathological conditions. Recently, a study showed that ROS produced by altered cancer cell metabolism or by treatment with drugs promotes autophagy and subsequent autophagic cell death [40]. Nevertheless, ROS generation was not induced by a 24-h treatment with BO-1051 in glioma cells (data not shown), suggesting that BO-1051-induced autophagy may not occur in an ROS-dependent manner, even though ROS are positive regulators of autophagy induction.

Treatment of malignant glioma is limited by the blood–brain barrier, which acts as a physiological barrier to drug delivery. Kapuriya et al. demonstrated that BO-1051 crosses the blood–brain barrier (data not shown) and suppresses cell growth in a human glioma U87MG xenograft model [4]. Because ionizing radiation remains the most consistently used therapy for patients with malignant glioma, we examined the effects of the combined treatment of BO-1051 and irradiation in glioma cells. We recently reported that BO-1051 effectively enhanced the radiosensitivity of glioma cells both in vitro and in vivo. Collectively, these results demonstrated that BO-1051 may serve as an adjuvant therapy to established chemotherapeutic drugs and/or radiation therapy.

In conclusion, the present study demonstrated that BO-1051 produces higher cytotoxicity against malignant glioma cells, which is accompanied by enhanced autophagic flux and caspase-dependent apoptosis. The cytoprotective role of BO-1051-induced autophagy was mediated through the down-regulation of Akt/mTOR and was associated with up-regulation of Erk1/2 activity. Inhibition of autophagy enhances BO-1051-induced apoptotic cell death in glioma cells. The identification of this pathway might elucidate the role of autophagy in anticancer treatment and suggests that BO-1051 could be an effective treatment for patients with malignant glioma.

**Acknowledgments** This study was supported by research grants from the National Science Council (NSC97-3111-B-075-001-MY3, NSC98-2320-B-075-003-MY3, NSC99-2628-B- 016-014-MY3 and NSC99-2811-B-016-007-MY3), Taipei Veterans General Hospital (V97B1-006 and E1-008, F-001), Tri-Service General Hospital (TSGH-C100-047), the Joint Projects of UTVGH (VGHUST 98-p1-01), Yen-Tjing-Ling Medical Foundation (96/97/98), National Yang-Ming University (Ministry of Education, Aim for the Top University Plan) & Genomic Center Project, Institute of Biological medicine, Academia Sinica (IBMS-CRC99-p01), and Center of Excellence for Cancer Research at Taipei Veterans General Hospital (DOH99-TD-C-111-007), Taiwan.

**Conflict of interest** None.

## References

1. Stupp R, Mason WP, van den Bent MJ, Weller M, Fisher B et al (2005) Radiotherapy plus concomitant and adjuvant temozolomide for glioblastoma. N Engl J Med 352:987–996
2. Rajski SR, Williams RM (1998) DNA cross-linking agents as antitumor drugs. Chem Rev 98:2723–2796
3. Maze R, Carney JP, Kelley MR, Glassner BJ, Williams DA et al (1996) Increasing DNA repair methyltransferase levels via bone marrow stem cell transduction rescues mice from the toxic effects of 1, 3-bis(2-chloroethyl)-1-nitrosourea, a chemotherapeutic alkylating agent. Proc Natl Acad Sci USA 93:206–210
4. Kapuriya N, Kapuriya K, Zhang X, Chou TC, Kakadiya R et al (2008) Synthesis and biological activity of stable and potent antitumor agents, aniline nitrogen mustards linked to 9-anilinoacridines via a urea linkage. Bioorg Med Chem 16:5413–5423
5. Su TL, Lin YW, Chou TC, Zhang X, Bacherikov VA et al (2006) Potent antitumor 9-anilinoacridines and acridines bearing an alkylating N-mustard residue on the acridine chromophore: synthesis and biological activity. J Med Chem 49:3710–3718
6. Su TL (2002) Development of DNA topoisomerase II-mediated anticancer agents, 3-(9-acridinylamino)-5-hydroxymethylanilines (AHMAs) and related compounds. Curr Med Chem 9:1677–1688
7. Chu PM, Chiou SH, Su TL, Lee YJ, Chen LH et al (2011) Enhancement of radiosensitivity in human glioblastoma cells by the DNA N-mustard alkylating agent BO-1051 through augmented and sustained DNA damage response. Radiat Oncol 6:7
8. Chen S, Rehman SK, Zhang W, Wen A, Yao L et al (2010) Autophagy is a therapeutic target in anticancer drug resistance. Biochim Biophys Acta 1806:220–229
9. Tiwari M, Bajpai VK, Sahasrabuddhe AA, Kumar A, Sinha RA et al (2008) Inhibition of N-(4-hydroxyphenyl)retinamide-induced autophagy at a lower dose enhances cell death in malignant glioma cells. Carcinogenesis 29:600–609
10. Shingu T, Fujiwara K, Bogler O, Akiyama Y, Moritake K et al (2009) Inhibition of autophagy at a late stage enhances imatinib-induced cytotoxicity in human malignant glioma cells. Int J Cancer 124:1060–1071
11. Kanzawa T, Germano IM, Komata T, Ito H, Kondo Y et al (2004) Role of autophagy in temozolomide-induced cytotoxicity for malignant glioma cells. Cell Death Differ 11:448–457
12. Lomonaco SL, Finniss S, Xiang C, Decarvalho A, Umansky F et al (2009) The induction of autophagy by gamma-radiation contributes to the radioresistance of glioma stem cells. Int J Cancer 125:717–722
13. Liu WT, Lin CH, Hsiao M, Gean PW (2011) Minocycline inhibits the growth of glioma by inducing autophagy. Autophagy 7:166–175
14. Alonso MM, Jiang H, Yokoyama T, Xu J, Bekele NB et al (2008) Delta-24-RGD in combination with RAD001 induces enhanced anti-glioma effect via autophagic cell death. Mol Ther 16:487–493
15. Chao AC, Hsu YL, Liu CK, Kuo PL (2011) alpha-Mangostin, a dietary xanthone, induces autophagic cell death by activating the AMP-activated protein kinase pathway in glioblastoma cells. J Agric Food Chem 59:2086–2096
16. Kondo Y, Kanzawa T, Sawaya R, Kondo S (2005) The role of autophagy in cancer development and response to therapy. Nat Rev Cancer 5:726–734

17. Eisenberg-Lerner A, Bialik S, Simon HU, Kimchi A (2009) Life and death partners: apoptosis, autophagy and the cross-talk between them. Cell Death Differ 16:966–975
18. Fu YS, Lin YY, Chou SC, Tsai TH, Kao LS et al (2008) Tetramethylpyrazine inhibits activities of glioma cells and glutamate neuro-excitotoxicity: potential therapeutic application for treatment of gliomas. Neuro Oncol 10:139–152
19. Paglin S, Hollister T, Delohery T, Hackett N, McMahill M et al (2001) A novel response of cancer cells to radiation involves autophagy and formation of acidic vesicles. Cancer Res 61:439–444
20. Chen LH, Loong CC, Su TL, Lee YJ, Chu PM et al (2011) Autophagy inhibition enhances apoptosis triggered by BO-1051, an N-mustard derivative, and involves the ATM signaling pathway. Biochem Pharmacol 81:594–605
21. Jinno-Oue A, Shimizu N, Hamada N, Wada S, Tanaka A et al (2010) Irradiation with carbon ion beams induces apoptosis, autophagy, and cellular senescence in a human glioma-derived cell line. Int J Radiat Oncol Biol Phys 76:229–241
22. Kanzawa T, Kondo Y, Ito H, Kondo S, Germano I (2003) Induction of autophagic cell death in malignant glioma cells by arsenic trioxide. Cancer Res 63:2103–2108
23. Bursch W, Ellinger A, Kienzl H, Torok L, Pandey S et al (1996) Active cell death induced by the anti-estrogens tamoxifen and ICI 164 384 in human mammary carcinoma cells (MCF-7) in culture: the role of autophagy. Carcinogenesis 17:1595–1607
24. Fu J, Shao CJ, Chen FR, Ng HK, Chen ZP (2010) Autophagy induced by valproic acid is associated with oxidative stress in glioma cell lines. Neuro Oncol 12:328–340
25. Mizushima N, Yoshimori T, Levine B (2010) Methods in mammalian autophagy research. Cell 140:313–326
26. Pankiv S, Clausen TH, Lamark T, Brech A, Bruun JA et al (2007) p62/SQSTM1 binds directly to Atg8/LC3 to facilitate degradation of ubiquitinated protein aggregates by autophagy. J Biol Chem 282:24131–24145
27. Shinojima N, Yokoyama T, Kondo Y, Kondo S (2007) Roles of the Akt/mTOR/p70S6K and ERK1/2 signaling pathways in curcumin-induced autophagy. Autophagy 3:635–637
28. Scarlatti F, Granata R, Meijer AJ, Codogno P (2009) Does autophagy have a license to kill mammalian cells? Cell Death Differ 16:12–20
29. Maiuri MC, Zalckvar E, Kimchi A, Kroemer G (2007) Self-eating and self-killing: crosstalk between autophagy and apoptosis. Nat Rev Mol Cell Biol 8:741–752
30. Levy JM, Thorburn A (2011) Targeting autophagy during cancer therapy to improve clinical outcomes. Pharmacol Ther 131:130–141
31. Das A, Banik NL, Patel SJ, Ray SK (2004) Dexamethasone protected human glioblastoma U87MG cells from temozolomide induced apoptosis by maintaining Bax:Bcl-2 ratio and preventing proteolytic activities. Mol Cancer 3:36
32. Haga N, Fujita N, Tsuruo T (2005) Involvement of mitochondrial aggregation in arsenic trioxide (As2O3)-induced apoptosis in human glioblastoma cells. Cancer Sci 96:825–833
33. Qian W, Liu J, Jin J, Ni W, Xu W (2007) Arsenic trioxide induces not only apoptosis but also autophagic cell death in leukemia cell lines via up-regulation of Beclin-1. Leuk Res 31:329–339
34. Zhang H, Kong X, Kang J, Su J, Li Y et al (2009) Oxidative stress induces parallel autophagy and mitochondria dysfunction in human glioma U251 cells. Toxicol Sci 110:376–388
35. Abedin MJ, Wang D, McDonnell MA, Lehmann U, Kelekar A (2007) Autophagy delays apoptotic death in breast cancer cells following DNA damage. Cell Death Differ 14:500–510
36. Ito H, Daido S, Kanzawa T, Kondo S, Kondo Y (2005) Radiation-induced autophagy is associated with LC3 and its inhibition sensitizes malignant glioma cells. Int J Oncol 26:1401–1410
37. Herman-Antosiewicz A, Johnson DE, Singh SV (2006) Sulforaphane causes autophagy to inhibit release of cytochrome C and apoptosis in human prostate cancer cells. Cancer Res 66:5828–5835
38. Harhaji-Trajkovic L, Vilimanovich U, Kravic-Stevovic T, Bumbasirevic V, Trajkovic V (2009) AMPK-mediated autophagy inhibits apoptosis in cisplatin-treated tumor cells. J Cell Mol Med 13:3644–3654
39. Sotelo J, Briceno E, Lopez-Gonzalez MA (2006) Adding chloroquine to conventional treatment for glioblastoma multiforme: a randomized, double-blind, placebo-controlled trial. Ann Intern Med 144:337–343
40. Dewaele M, Maes H, Agostinis P (2010) ROS-mediated mechanisms of autophagy stimulation and their relevance in cancer therapy. Autophagy 6:838–854